
PI-NAV: Physics-Informed Universal Differential Equations for Enhanced Nanorobot Navigation through Complex Bio-environments

Tarushri N S

Indian Institute of Science
Bengaluru, India
tarushrins@gmail.com

Prathamesh Dinesh Joshi

Vizuara AI Labs
121cs0072@iiitk.ac.in

Raj Abhijit Dandekar

Vizuara AI Labs
raj@vizuara.com

Rajat Dandekar

Vizuara AI Labs
rajatdandekar@vizuara.com

Sreedath Panat

Vizuara AI Labs
sreedath@vizuara.com

Abstract

Magnetically actuated nanoswimmers are emerging as promising agents for targeted drug delivery and minimally invasive biomedical operations. Modeling their motion through complex, heterogeneous extracellular environments remains a fundamental challenge: purely mechanistic models often fall short due to unknown extracellular matrix interactions while purely data driven models struggle with extrapolation and stability. We address this gap using a physics-informed Universal Differential Equation (UDE) based approach. Here, we have embedded a mechanistic backbone based on magnetic torque and low-Reynolds propulsion into a learnable neural residual, training the system to accurately capture unknown environmental forces from observed trajectories. On a synthetic navigation task with a Gaussian barrier, the UDE performs brilliantly achieving a total root-mean-squared error (RMSE) of 0.015, compared to 2.52 for physics-only and 0.285 for a purely neural ODE. Untrained UDEs diverged with RMSE 12.95. These results highlight the strong accuracy, stability, and data-efficiency of physics-guided learning. More broadly, this work positions physics-informed UDEs as a compact and interpretable framework for modeling complex biophysical systems, advancing the role of scientific machine learning in biomedical micro/nano-robotics.

1 Introduction

Magnetically actuated nanoswimmers are at the forefront of biomedical micro/nano-robotics, enabling applications such as targeted drug delivery, minimally invasive surgery, and magnetic hyperthermia therapy [Nelson et al., 2010, Li et al., 2017, Sitti et al., 2015, Wang et al., 2017]. Their nanoscale dimensions, biocompatibility, and ability to be remotely steered by oscillating magnetic fields make them ideally suited for navigating extracellular matrices (ECM) and vascular microenvironments [Abbott et al., 2009, Gao and Wang, 2014]. However, accurately modeling their dynamics in such environments remains profoundly challenging: while low-Reynolds-number (low-Re) hydrodynamics is well understood [Purcell, 1977, Lauga and Powers, 2009], real biological environments introduce heterogeneous barriers, anisotropic drag, and hydrodynamic coupling that are difficult to parametrize [Fauci and Dillon, 2006, Elgeti et al., 2015].

Purely mechanistic models, based on Stokes flow and magnetic torque, capture propulsion and viscous damping but fail to represent ECM-induced deflections or localized anisotropy [Ishimoto

and Gaffney, 2014, Marcos et al., 2012]. In our Gaussian barrier navigation benchmark, such a physics-only model exhibits a trajectory root-mean-squared error (RMSE) of **2.52** over positions and velocities, underscoring its predictive limitations. In contrast, purely data-driven approaches such as Neural Ordinary Differential Equations (Neural ODEs) can approximate nonlinear force fields [Chen et al., 2018, Dupont et al., 2019], but they generalize poorly, exhibit instability under sparse data, and lack interpretability [Kidger, 2022, Rackauckas et al., 2020, Kim et al., 2021]. In our experiments, a black-box neural ODE achieved RMSE **0.285**, improving over physics-only but still insufficient for biomedical deployment.

Physics-informed machine learning offers a principled middle ground by embedding known physical laws into trainable residuals [Raissi et al., 2019, Karniadakis et al., 2021]. Universal Differential Equations (UDEs) formalize this approach by coupling mechanistic backbones with neural components, enabling the recovery of “missing physics” while preserving inductive bias from theory [Rackauckas et al., 2020, Kim et al., 2021]. Applied to nanoswimmer navigation, this hybridization yields striking accuracy: our trained UDE achieves a total RMSE of **0.015**, using only a single training trajectory. These results highlight the data-efficiency, robustness, and interpretability of physics-guided learning in micro/nano-scale biophysics.

2 Methodology

2.1 Synthetic data generation

To evaluate different modeling approaches under controlled conditions, we generated synthetic trajectories of a nanoswimmer navigating a 2D ECM environment, simulated using a Gaussian barrier potential centered at (5,5), representing a repulsive ECM obstacle:

$$U(x, y) = U_0 \exp\left(-\frac{(x - x_0)^2 + (y - y_0)^2}{2\sigma^2}\right), \quad (1)$$

with U_0 the barrier strength, (x_0, y_0) the center, and σ the spread. Such Gaussian barriers approximate localized ECM obstacles like fibrous nodes or protein aggregates [Fauci and Dillon, 2006, Elgeti et al., 2015].

We solved this “truth system” using the Tsitouras 5/4 Runge–Kutta scheme [Tsitouras, 2011] implemented in `DifferentialEquations.jl` [Rackauckas and Nie, 2017], with fixed step size $\Delta t = 0.1$ s over a 50 s horizon. This yields ground-truth trajectories $\{x(t), y(t), v_x(t), v_y(t)\}$ used for supervised training.

2.2 Physical model and UDE formulation

The swimmer was actuated by a rotating magnetic field $\mathbf{B}(t) = B_0 [\cos(\omega t), \sin(\omega t), 0]^\top$, interacting with a fixed body dipole moment $\mathbf{m} = [0, 0, 1]^\top$ to produce torque $\boldsymbol{\tau}(t) = \mathbf{m} \times \mathbf{B}(t)$. Propulsion is assumed to be aligned with the body axis (\hat{y}), with magnitude proportional to torque norm, $\mathbf{F}^{\text{prop}} = \alpha \|\boldsymbol{\tau}(t)\| \hat{y}$ where α is a tunable propulsion gain, and \mathbf{F}^{prop} is the propulsion force induced by $\mathbf{B}(t)$. This abstraction captures magnetic drive fidelity while eliminating explicit rotational states, consistent with prior low-Re models [Purcell, 1977, Lauga and Powers, 2009].

The swimmer’s state $\mathbf{u} = [x, y, v_x, v_y]^\top \in \mathbb{R}^4$ evolves under low-Re dynamics:

$$\begin{aligned} \dot{x} &= v_x, & \dot{y} &= v_y, \\ \dot{v}_x &= -\partial_x U(x, y) - \eta v_x + F_x^{\text{prop}}(t), & \dot{v}_y &= -\partial_y U(x, y) - \eta v_y + F_y^{\text{prop}}(t). \end{aligned} \quad (2)$$

Here, η is the damping coefficient representing viscous drag. Following [Purcell, 1977, Lauga and Powers, 2009], we assume inertia is negligible, and mass is normalized into coefficients. This system is analytically tractable only when $U(x, y)$ is known, which is rarely the case in real ECM environments. To overcome this, we replace $\nabla U(x, y)$ with a learnable residual $\widehat{\nabla U}(x, y, t)$ parameterized by a neural network, producing a Universal Differential Equation (UDE) [Rackauckas et al., 2020, Kim et al., 2021]. This preserves physical structures like propulsion and drag, while flexibly modeling unknown interactions.

2.3 Training and optimization

We train the UDE by minimizing a loss function which is the mismatch between simulated rollouts and ground-truth trajectories:

$$\mathcal{L}(\theta) = \sum_k \|\hat{\mathbf{u}}(t_k; \theta) - \mathbf{u}_{\text{true}}(t_k)\|_2^2, \quad (3)$$

where θ are network parameters, \mathbf{u}_{true} is the synthetic trajectory, and $\hat{\mathbf{u}}$ is the model prediction at time t_k . Loss gradients were computed via adjoint sensitivity analysis [Chen et al., 2018, Ma et al., 2018] using Zygote VJP[Innes, 2018]. Table 1 summarizes the network architecture and training setup.

Table 1: Network architecture and training hyperparameters for the navigation task.

Component	Specification
<i>Network Architecture</i>	
Input layer	3 neurons (x, y, t)
Hidden layer 1	32 neurons, tanh activation
Hidden layer 2	32 neurons, tanh activation
Output layer	2 neurons ($\widehat{\nabla U_x}, \widehat{\nabla U_y}$), linear
<i>Training and Optimization</i>	
Optimizer (Phase I)	ADAM, learning rate = 0.01, 7500 iterations
Optimizer (Phase II)	L-BFGS (OptimJL), 500 iterations
Loss function	Trajectory MSE over $[x, y, v_x, v_y]$
ODE solver	Tsit5 (5th-order Runge–Kutta)
Step size Δt	0.1 s, total time = 50 s
ODE tolerance (abs/rel)	$10^{-6} / 10^{-6}$
Sensitivity method	Interpolating Adjoint (Zygote VJP)
Parameter dtype	Float32, seed = 42

3 Results

3.1 Training dynamics

The UDE residual network was trained with ADAM (7,500 steps) followed by L-BFGS (500 steps). The training loss decreased from $\approx 3.9 \times 10^4$ at initialization to $\approx 4.5 \times 10^{-1}$ at convergence (Figure 1c), spanning nearly five orders of magnitude. The ADAM phase produces rapid variance reduction, while the quasi-Newton refinement stabilizes residual corrections, consistent with optimizer dynamics reported in prior neural ODE training studies [Chen et al., 2018, Dupont et al., 2019]. Small oscillations in the log-scale loss reflect moment-based updates [Kingma and Ba, 2015, Liu and Nocedal, 1989].

3.2 Trajectory reconstruction

Figures 1a–b compare ground truth trajectories with UDE rollouts. The untrained UDE diverges catastrophically, producing spurious downward turns (RMSE = 12.95), whereas the trained UDE overlaps almost perfectly with the ground truth (RMSE = 0.015). This corresponds to an **863**× improvement relative to the uninitialized network. In comparison, the physics-only baseline achieves RMSE = 2.52, and the neural network only (NN-only) model achieves 0.285, confirming that hybridization with physics priors dramatically improves generalization. Such behavior aligns with recent findings that physics-informed models reduce error accumulation in long-horizon rollouts [Rackauckas et al., 2020, Raissi et al., 2019].

3.3 Velocity transients

Figures 1d–e show velocity components under untrained vs trained models. The trained UDE reproduces both the amplitude and phase of the transient spike around $t \approx 15$ –20 s, followed by

viscous decay, capturing both v_x and v_y with high fidelity (RMSE: $v_x = 0.017$, $v_y = 0.017$). In contrast, the untrained UDE misses both the sign and amplitude of transients, consistent with the instability of unconstrained neural ODE residuals [Kidger, 2022]. The NN-only model (graphs not shown for brevity, refer table2 for data) tracked coarse trajectory trends but exhibited phase drift and amplitude mis-scaling in the velocity domain, further highlighting the stabilizing effect of embedding propulsion and drag [Purcell, 1977, Lauga and Powers, 2009].

3.4 RMSE ablation study

Table 2 summarizes errors across baselines. Relative to physics-only, the trained UDE reduces total RMSE from 2.52 to 0.015 (a $167\times$ improvement). Position-only RMSE drops from 3.53 to 0.0126 (99.6% reduction). Relative to NN-only, error is reduced from 0.285 to 0.015 (a $19\times$ improvement). This confirms that physics-guided learning provides both data efficiency and stability, consistent with broader reports in physics-informed machine learning [Karniadakis et al., 2021, Ma et al., 2018].

Table 2: RMSE comparison across models. Errors reported over rollout trajectories.

Model	x	y	v_x	v_y	Total RMSE
Physics-only	4.34	2.46	0.49	0.39	2.52
NN-only	0.27	0.27	0.32	0.28	0.285
UDE (untrained)	3.71	25.61	0.59	0.97	12.95
UDE (trained)	0.012	0.013	0.017	0.017	0.015

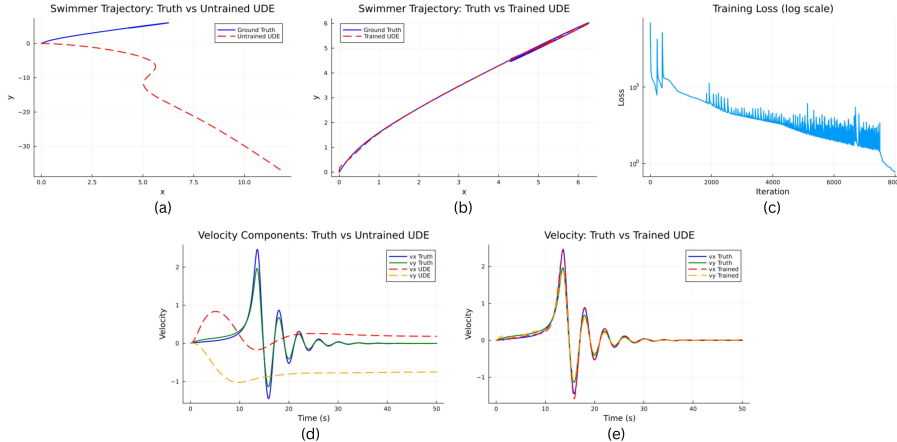


Figure 1: (a) Trajectory: truth vs untrained UDE. (b) Trajectory: truth vs trained UDE. (c) Training loss (log scale). (d) Velocity: truth vs untrained UDE. (e) Velocity: truth vs trained UDE.

4 Discussion and Conclusion

This work demonstrates that embedding physical priors into neural differential equations yields dramatic performance gains in nanoswimmer navigation. Our results provide compelling evidence that physics-informed architectures can combine interpretability, stability, and data efficiency which are the key requirements for real biomedical micro/nano-robotics [Nelson et al., 2010, Li et al., 2017].

Beyond trajectory reproduction, symbolic regression can extract analytic approximations of the residual dynamics, potentially rediscovering underlying force laws from the ECM [Brunton et al., 2016, Champion et al., 2019]. Robustness to extrapolation and long-horizon forecasting, a known limitation of black-box models [Kidger, 2022], can be systematically evaluated within this hybrid framework. Furthermore, the same UDE scaffold naturally extends to bioheat modeling via the Pennes equation [Pennes, 1948, Dutz and Hergt, 2014], enabling physics-informed optimization of

magnetic hyperthermia protocols. Such extensions highlight the generalizability of UDEs across biomedical tasks where physics is known but incomplete.

In conclusion, PI-NAV offers a compact and interpretable modeling paradigm that unifies mechanistic fidelity with the adaptability of deep learning. By achieving order-of-magnitude error reductions while preserving physical structure, our results establish physics-guided machine learning not merely as a modeling tool, but as an enabling technology for the next generation of micro/nano-robotics in medicine [Karniadakis et al., 2021, Rackauckas et al., 2020].

Broader Impact

Physics-informed machine learning frameworks such as PI-NAV have the potential to advance safe and effective biomedical micro/nano-robotics. Improved accuracy and stability in nanoswimmer navigation could accelerate progress in targeted drug delivery and minimally invasive therapies, ultimately reducing treatment risks and side effects. At the same time, as with any biomedical technology, careful consideration of safety, regulatory pathways, and equitable access will be essential to ensure that these advances translate into positive societal outcomes.

Post-Review Addendum: Clarifications and Discussion

1. Scope and Claims: Reviewers noted that our current evaluation relies on a controlled synthetic benchmark and therefore cannot support broad claims of biomedical deployment. We agree, and explicitly position PI-NAV as a *proof-of-concept* demonstration of how physics-informed Universal Differential Equations (UDEs) can stabilize and improve nanoswimmer trajectory prediction when only partial physics is known. The present study focuses on a simple and interpretable 2D Gaussian barrier to isolate the effect of the hybrid architecture and evaluate failure modes of physics-only or NN-only baselines. This setting establishes foundational behavior before extending to realistic ECM geometries or experimental systems. Future work will incorporate multi-barrier ECM fields, anisotropic drag, stochastic fluctuations, and experimental trajectories.

2. Motivation for Learning the Force Field $\nabla\hat{U}$ Directly: We directly learn the environmental force field $\nabla\hat{U}(x, t)$ rather than modeling a scalar potential $\hat{U}(x, t)$ and differentiating it. This choice is motivated by: (i) *Biophysical realism*: ECM-induced resistance is not strictly conservative; anisotropy, poroelasticity, and shear-dependent drag produce non-potential, path-dependent forces. Direct field learning avoids imposing incorrect conservative-force assumptions. (ii) *Numerical stability*: Differentiating a learned potential introduces second-order derivatives in the ODE adjoint calculation, often causing stiffness and unstable gradients. Directly predicting $\nabla\hat{U}$ empirically yields smoother optimization. (iii) *Interpretability*: The learned field can be visualized directly as a vector map of environmental influence. (iv) *Scientific ML precedent*: Many hybrid models treat unresolved physical effects as learned vector fields.

3. Interpretability: Reviewers noted that interpretability was stated but not sufficiently demonstrated. PI-NAV offers *structural interpretability* via the decomposition

$$\mathbf{a}(x, v, t) = \mathbf{F}_{\text{prop}}(t) - \nabla\hat{U}(x, t) - \eta v,$$

which forces the model to attribute deviations from known physics solely to the learned residual field, rather than absorbing them into a monolithic neural network. The residual is spatially localized around the barrier, smooth, and consistent with physical intuition. The observed stability improvement (e.g., avoidance of untrained UDE divergence) directly reflects interpretable inductive bias. Future work will add symbolic regression, vector-field visualizations and sensitivity analyses of $\nabla\hat{U}$.

4. Synthetic-Only Validation and Robustness: We acknowledge that evaluation on a single synthetic trajectory limits generality. Our aim was to isolate the effect of physics-guided learning on stability in a controlled environment. Future extensions will include multiple trajectories, noisy ECM fields, out-of-distribution rollouts, and validation using real nanoswimmer trajectories from magnetic or magnetic-acoustic actuation experiments.

We thank all reviewers for recognizing the value of hybrid UDE modeling for biophysical systems. We have clarified interpretability, modeling assumptions, and scope; and reframed claims to reflect the proof-of-concept nature of this work. These revisions strengthen the paper and offer a clear path toward future experimental and robustness-oriented extensions.

References

- Jake J Abbott, Kathrin E Peyer, Michele Cosentino Lagomarsino, Li Zhang, Lixin Dong, Ioannis K Kaliakatsos, and Bradley J Nelson. How should microrobots swim? *The International Journal of Robotics Research*, 28(11-12):1434–1447, 2009.
- Steven L Brunton, Joshua L Proctor, and J Nathan Kutz. Discovering governing equations from data by sparse identification of nonlinear dynamical systems. *Proceedings of the National Academy of Sciences*, 113(15):3932–3937, 2016.
- Kathleen Champion, Bethany Lusch, J Nathan Kutz, and Steven L Brunton. Data-driven discovery of coordinates and governing equations. *Proceedings of the National Academy of Sciences*, 116(45):22445–22451, 2019.
- Ricky T. Q. Chen, Yulia Rubanova, Jesse Bettencourt, and David Duvenaud. Neural ordinary differential equations. In *Advances in Neural Information Processing Systems (NeurIPS)*, pages 6571–6583, 2018.
- Emilien Dupont, Arnaud Doucet, and Yee Whye Teh. Augmented neural odes. In *Advances in Neural Information Processing Systems (NeurIPS)*, pages 3140–3150, 2019.
- Silvio Dutz and Robert Hergt. Magnetic nanoparticle heating and heat transfer on a microscale: Basic principles, realizations and biomedical applications. *International Journal of Hyperthermia*, 29(8):790–800, 2014.
- Jens Elgeti, Roland G Winkler, and Gerhard Gompper. Physics of microswimmers—single particle motion and collective behavior. *Reports on Progress in Physics*, 78(5):056601, 2015.
- Lisa J Fauci and Richard Dillon. Biofluidmechanics of reproduction. *Annual Review of Fluid Mechanics*, 38:371–394, 2006.
- Wei Gao and Joseph Wang. Synthetic micro/nanomotors in drug delivery. *Nanoscale*, 6(18):10486–10494, 2014. doi: 10.1039/C4NR03124E.
- Michael Innes. Don’t unroll adjoint: Differentiating ssa-form programs. *arXiv preprint arXiv:1810.07951*, 2018. <https://github.com/FluxML/Zygote.jl>.
- Kenta Ishimoto and Eamonn A Gaffney. Squirm dynamics near a boundary. *Physical Review E*, 90(1):012704, 2014.
- George E Karniadakis, Ioannis G Kevrekidis, Lu Lu, Paris Perdikaris, Sifan Wang, and Liu Yang. Physics-informed machine learning. *Nature Reviews Physics*, 3(6):422–440, 2021.
- Patrick Kidger. On neural differential equations. *Journal of Machine Learning Research*, 23(79):1–81, 2022.
- Suyong Kim, Weiqi Ji, Sili Deng, Yingbo Ma, and Christopher Rackauckas. Stiff neural ordinary differential equations. *Chaos*, 31(9):093122, September 2021. doi: 10.1063/5.0060697.
- Diederik P Kingma and Jimmy Ba. Adam: A method for stochastic optimization. In *International Conference on Learning Representations (ICLR)*, 2015.
- Eric Lauga and Thomas R Powers. The hydrodynamics of swimming microorganisms. *Reports on Progress in Physics*, 72(9):096601, 2009.
- Jinxing Li, Berta Esteban-Fernández de Ávila, Wei Gao, Li Zhang, and Joseph Wang. Micro/nanorobots for biomedicine: Delivery, surgery, sensing, and detoxification. *Science Robotics*, 2(4):eaam6431, 2017.

- Dong C. Liu and Jorge Nocedal. On the limited memory bfgs method for large scale optimization. *Mathematical Programming*, 45(1-3):503–528, 1989.
- Yingbo Ma, Vaibhav Dixit, Mike Innes, Xingjian Guo, and Christopher Rackauckas. A comparison of automatic differentiation and continuous sensitivity analysis for derivatives of differential equation solutions. arXiv preprint arXiv:1812.01892, 2018. Available at <https://arxiv.org/abs/1812.01892>.
- Marcos, Henry C Fu, Thomas R Powers, and Roman Stocker. Bacterial rheotaxis. *Proceedings of the National Academy of Sciences*, 109(13):4780–4785, 2012.
- Bradley J Nelson, Ioannis K Kaliakatsos, and Jake J Abbott. Microrobots for minimally invasive medicine. *Annual Review of Biomedical Engineering*, 12:55–85, 2010.
- Harry H Pennes. Analysis of tissue and arterial blood temperatures in the resting human forearm. *Journal of Applied Physiology*, 1(2):93–122, 1948.
- Edward M Purcell. Life at low reynolds number. *American Journal of Physics*, 45(1):3–11, 1977.
- Chris Rackauckas, Yingbo Ma, Julius Martensen, Christopher Warner, Kirill Zubov, Rohit Supekar, Dominic Skinner, Ali Ramadhan, and Alan Edelman. Universal differential equations for scientific machine learning. *Proceedings of the National Academy of Sciences*, 117(15):8490–8500, 2020.
- Christopher Rackauckas and Qing Nie. Differentialequations.jl—a performant and feature-rich ecosystem for solving differential equations in julia. *Journal of Open Research Software*, 5(1), 2017.
- Maziar Raissi, Paris Perdikaris, and George E Karniadakis. Physics-informed neural networks: A deep learning framework for solving forward and inverse problems involving nonlinear pdes. *Journal of Computational Physics*, 378:686–707, 2019.
- Metin Sitti, Hakan Ceylan, Wenqi Hu, James Giltinan, Mehmet Turan, Sungwhan Yim, and Eric Diller. Biomedical applications of untethered mobile milli/microrobots. *Proceedings of the IEEE*, 103(2):205–224, 2015.
- Ch Tsitouras. Runge–kutta pairs of order 5(4) satisfying only the first column simplifying assumption. *Computers & Mathematics with Applications*, 62(2):770–775, 2011.
- Ben Wang, Kostas Kostarelos, Bradley J Nelson, and Li Zhang. Trends in micro-/nanorobotics: biomedical applications. *Materials Today*, 19(3):163–171, 2017.